3-D Image Modeling and Shape Reconstruction of Electrical Discharges using Computer Vision

Mathini Sellathurai
Dept. of Electric Power Engineering
Royal Institute of Technology
Stockholm, Sweden

Fredrik Bergholm
Dept. of Numerical Analysis and Computing Sc.
Royal Institute of Technology
Stockholm, Sweden

Abstract

In this paper, a new measurement approach in high voltage engineering is proposed using computer vision for constructing the 3-D shape of electrical discharges. Eventually the method finds the orientation of the channel sections. This paper addresses a computationally inexpensive problem oriented algorithm to reconstruct 3-D points of electrical discharges from two simultaneous image pairs without knowing point to point correspondences. We assume roughly parallel optical axes, but the epipolar lines are not assumed to be known. By minimizing sum of squared disparity differences (SSDD) of neighborhood features, a robust estimate for correspondence and vertical misalignment of cameras are obtained in the laboratory and outdoor measurements. A detailed light analysis and the image formation model for the light emitting discharges (typically for a light source) are derived by using the observed characteristics and are incorporated in the image matching algorithm. The experimental results are presented demonstrating the ability of the technique to recover the 3-D shape of the electrical discharges.

1 Introduction

A reliable power supply is becoming increasingly important to modern society as electronics are being introduced into more and more fields, thus demanding a higher protection from electrical hazards. The main causes of these electrical hazards are high voltage electrical discharges such as lightning, sparks and surface discharges. One of the challenges in discharge research is to find the direction of propagation of the current, i.e., the orientation of the return stroke channel sections. The time taken for a discharge phenomenon is a few tens of milliseconds to a few hundreds of milliseconds and measuring the 3-D path by any measuring method is difficult in practice [3]. So far, there are no methods available for direct measurements of the geometry of electrical discharges. This paper contributes by a systematic and general methodology for analysis the zigzag channels of electrical discharges in 3-D using stereo imaging techniques, also discussing possible ways to match image formation.

In this paper, an experimental technique and the step-by-step approach carried out for reconstructing the 3-D shape of laboratory discharges from 2-D binocular parallel camera images are presented. The estimated 3-D structure was verified by a third camera, fixed orthogonal to the line-of-sight of the first two cameras (a ground truth for depth in discharge images). A very basic problem in image analysis is developing the algorithms for the given task. The image analysis of each and every image varies according to its characteristics. We present a new problem-oriented image matching algorithm which uses the light characteristics of the discharge images modeled in section 4. The algorithm is computationally inexpensive compared to the intensity-based matching algorithms [1]. Finally the experimental results are presented.

2 Experimental set-up

Three calibrated cameras (lenses with 28 mm focal length) were placed as shown in Fig. 1. The first two cameras are parallel to each other and the third camera was placed orthogonal to the first two cameras. The high voltage laboratory was darkened and the cameras were triggered simultaneously to image the discharges. The discharges were generated in a 2.1 m vertical rod-plane gap, [6].

We denote orientation of each channel section modeled as (θ^*, φ), slope and azimuth angle respectively. When we measure from the point P, the slope of section BC is the angle between the channel section and the vertical (Y) axis (Fig. 2). A set of images captured by the three cameras (Fig. 1) is shown in Fig. 3. The discharges are single channel spans in 3-D space and discharge images are thin and bright glow on a dark background. The image taken by Camera 3 is called *orthogonal picture*

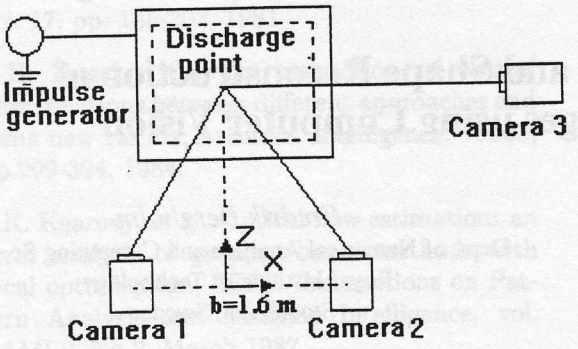

Fig. 1 View from above of the imaging set up

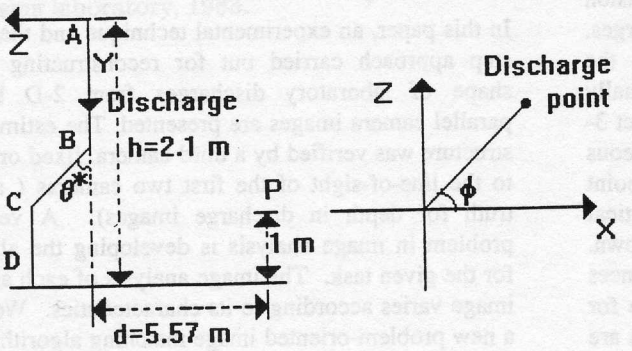

Fig. 2 The orientation of an electrical discharge from measuring point P.

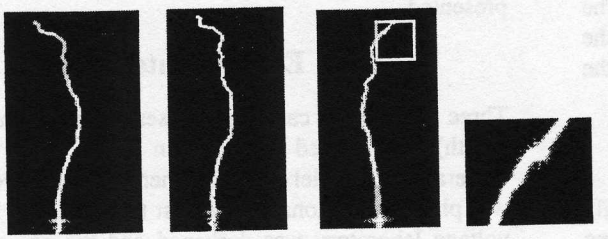

(a) Camera 1 (b) Camera 2 (c) Camera 3 (d) Highlighted part of Camera 3

Fig. 3 Simultaneous images from a typical experiment

3 Shape analysis using light characteristics

The type of light falling on an object, and the characteristics of the object itself largely determines the image formation of an opaque non-illuminating objects. Electrical discharge is an object which emits light itself. The characteristics of the illumination function of a discharge image is different from that of reflecting surfaces. For the interest of the reader, some observed characteristics are explained.

Intensity values: A characteristic example of the pixel intensity values of highlighted part of the channel shown in Fig. 3(a) is given below.

The brightness of the discharge image is caused by high current flow along the channels. The bright part of the channel is 1-3 pixels wide and it behaves more or less like a one to three pixel wide bright wire, on a dark background.

Table 1: Intensity values- an example (8 bit image)

82	219	256	256	236	22	45	42
82	73	242	256	250	116	34	45
79	14	236	256	250	72	31	42
58	14	227	256	256	146	14	42
58	63	188	256	256	190	7	42
44	14	188	256	256	146	14	45

Light variation across the channel and the shape of discharge cross sections: Figs. 4 shows the intensity distribution across the channel at correspondence points from three different directions.

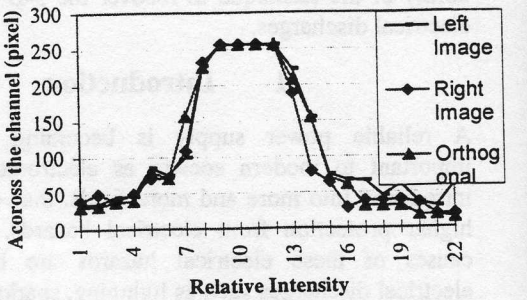

Fig. 4 Intensity profile along the row from three different directions at matched pixels for images in Fig. 3.

The peak points obtained from any direction will go through the center of the cross section because the shape of the lightning is volumetric and cylindrical. The intensity profile is quite symmetric and similar for all

three view points (= all three cameras) in many sections which is an indication of the channels behaving as cylindrical emitters.

Light blob at a depth discontinuity: A bright spot is observed in the *orthogonal picture* at a depth discontinuity along the visual rays (intensity change due to orientation). The bright spot is due to additivity of light, at the depth discontinuity in the direction of line of sight (transparency). In Fig. 3(c), the bright spot is slightly visible (highlighted by a frame) and the corresponding depth discontinuity is visible in the images 3(a) and (b). Fig. 3(d) shows the zoomed part highlighted in Fig. 3(c). The bright blob is clearly visible in 3(d).

4 Modeling of discharge images related to shape of the channels

In physics a channel is modeled as cylindrical or spherical short sections. The so-called tortuosity of the channel is divided into macro and micro level [3]. Macro tortuosity refers to the major channel segments. A tortuosity of much smaller scale imposed over the channel is called micro tortuosity. As mentioned, in our case the height of the discharge is 2.1 m in laboratory experiments. The macro tortuosity can be taken as short as tens of centimeters.

The glowing channel is modeled as a finite number of isotropic point sources located in a cylindrical tube of constant radius, consisting of sections of 3D-orientations specified by the polar (slope) angle θ^* and the azimuth angle φ. We now derive an image formation model. Denote the number of light sources per volume in a narrow cylindrical section perpendicular to the tube spine of the channel by S. Fig. 5 shows visual rays intersecting a cylindrical subsection.

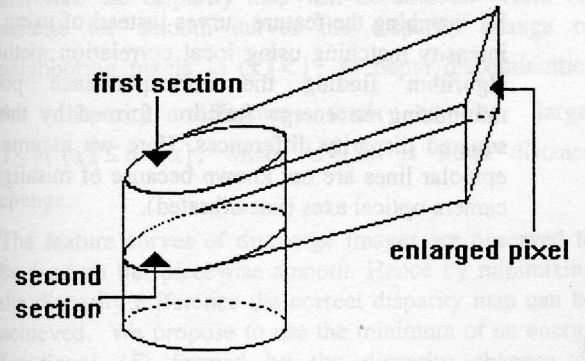

Fig. 5 Visual rays in section planes, intersecting a cylindrical tube.

Case I, Fig. 6: The number of light sources involved in forming the brightness at a certain pixel is dependent on the sections between the planes spanned by two pairs of nearby visual rays (say at either side of the pixel, Fig. 5) and the cylindrical channel tube. The corresponding light collected by a lens is

$$L_1 = C_1 \cdot S \Big/ \left(\cos\theta \cdot d^2\right) \quad W / \left(m^2 \times sr\right) \tag{1}$$

where $d = z / cos(\alpha)$ is the distance to the channel, α is the angle between optical axis and visual ray direction, C_1 is a constant, and θ the angle between current section normal and the cylindrical spine. Equation (1) turns into the brightness

$$I_1 = C_1 \cdot \frac{S \cdot Z^2}{\cos\theta \cdot d^2} \quad W / m^2 \tag{2}$$

of the pixel.

The formula applies, unless the angle θ is close to 90° so that the channel sections have changed direction appreciably (case II, Fig. 6). We stress that the unit of the outgoing light cone is W per m^2 and steradians, but the generating region is the channel volume behind a pixel rectangle, projected (by perspective projection) onto the image.

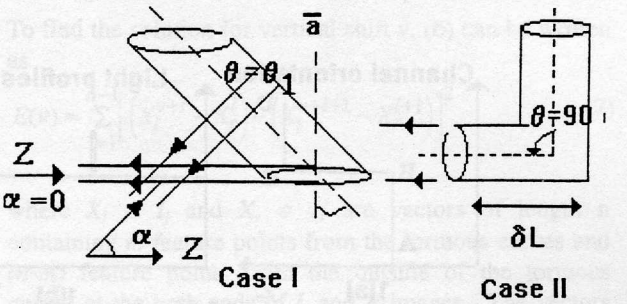

Fig. 6 Cylindrical channel section. Case I: Here, $\theta = \theta_1 = 0$ for the section between visual rays and the tube in direction α. Visual rays normal to $\bar{a}$ have $\theta = \theta_0$. *Case* II: Aligned local section, $\theta = 90°$, θ is the angle between the cylindrical tube spine and a normal to the section.

Case II, Fig. 6: Another similar effect is assumed to appear when the channel is aligned with the visual ray. (For the midpoint of the image, the channel is horizontal). Then the number of light sources N involved in creating

the brightness is assumed to be proportional to the length δL of the aligned local channel section, where $N = S \cdot \delta L$. The brightness in the image is

$$I_2 = C_2 \cdot \frac{N \cdot Z^2}{d^2} \qquad W/m^2 \qquad (3)$$

where C_2 is a constant. See also Fig. 6.1(b).

The formulas (2) and (3) are thought of as being more or less mutually exclusive. When the channel is approximately aligned to the visual ray, (3) holds, otherwise (2).

Both (2) and (3) are effectively depending on additivity of light sources in a **volume**, but different sections are involved. For data towards the edge of the image, more cosine effects should be added, due to oblique light cones and image plane main message is that this simple image formation orientation [2].

Anyway, the hypothesis predicts a sharp intensity increase close to a distance discontinuity (= when the visual ray aligned to the direction of the channel). This is shown in Fig. 7.1.

Sharp intensity increases could, in theory, also appear if the channel forms a sharp (90 degrees tilted) V. In Fig. 7.2, a not so sharp V-shape is shown. For a distance discontinuity, this prediction is in accordance with *measurements* as mentioned in Section 3.

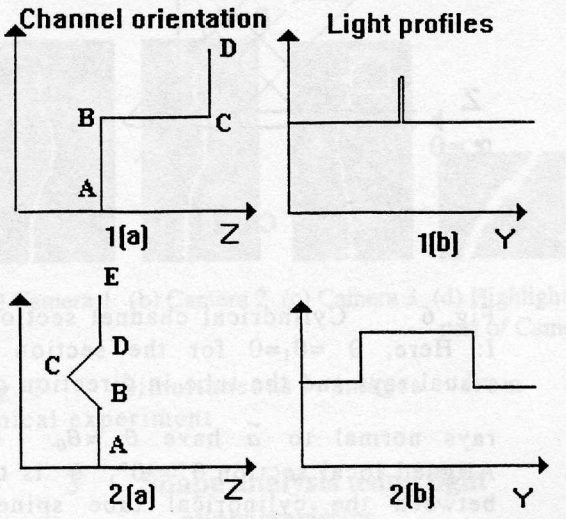

Fig. 7 Light profile expected for the channel orientations given.

5 Feature Extraction

A 3-D scene can be segmented using different cues, such as boundaries, texture, motion, optical flow discontinuities etc.. In motion analysis, optical flow discontinuities complicate the task of segmentation in reflecting (non-illuminating) objects because of shadows. Here using binocular image pairs, disparity flow[1] is a prominent feature and used in channel segmentation.

The light illumination occurs in the channel because of the current flow between the electrodes. As a good approximation, the current path can be assumed to be along the maximum (saturated ≈ 256) intensity of the channel. Therefore, the path selected along the peak intensity points of left and right images are the corresponding points representing current path in world coordinates. We call this the peak glow path. For a low resolution picture (400 by 400 pixels) the saturated part of the high-intensity glow is observed in one pixel thickness most of the time. For a higher resolution picture (1028 by 1028), the saturation is observed for more than one pixel thickness. In this case, the center points are assumed as the center of the circular sections. In this approach we take only one feature for one row. At horizontal sections of the channel, the algorithm (described below) takes only one sample point at the middle of the section.

6 Image matching algorithm

Discharge images are not binary images but the peak glow path is quite a prominent feature. Hence, the discharge channel is an almost ideal feature in the sense that it is easily detectable and often there is only one matching candidate per image row, in stereo matching pairs. It is quite advantageous to omit gray values in the matching stage since the channel ridge is a really well-localized clear feature and the gray value contains little information. A global matching technique is proposed for matching the feature curves instead of using the light intensity matching using local correlation methods. The algorithm finding the correspondence points by minimizing an energy function formed by the sum of squared disparity differences. Here we assume that the epipolar lines are not known because of misalignment of camera optical axes (uncalibrated).

[1] Which is a kind of analogue to optical flow, comparing static and dynamic binocular image pairs

6.1 Disparity difference

Fig. 8 shows the camera geometry for two parallel cameras L and R. The object points P_1, P_2 are projecting the two neighboring pixels p_1, p_2 in left and right images.

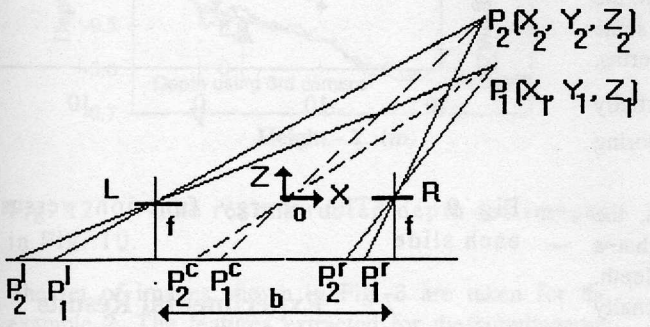

Fig. 8 Definition of disparity difference for parallel binocular stereo geometry.

In the case of parallel binocular stereo, the vertical disparity is 0, i.e., $y_l = y_r$ so that $y_l - y_r = 0$. The horizontal disparity d

$$d = x_l - x_r = bf/Z \tag{4}$$

The disparity change for two given neighboring points (first derivative of disparity) P_1 $(=(X_1, Y_1, Z_1))$ and P_2 $(=(X_2, Y_2, Z_2))$ is given by the difference in disparities d'

$$d' = |d_2 - d_1| \tag{5}$$

For a smooth surface or a curve, the depth of the surface or curve is smooth. Disparity is a function of depth, therefore the disparity map will be smooth. Here we assume for smooth curves the disparity change of neighboring pixels $|d'(x)| < 1$. At depth discontinuities the disparity difference tends to be large, $1 < |d'(x)| \le d^*(x)$, where $d^*(x)$ is finite distance change.

The feature curves of discharge images are observed to be random but piecewise smooth. Hence by minimizing the disparity difference the correct disparity map can be achieved. We propose to use the minimum of an energy functional (E) formed by the disparity changes of neighboring feature pixels(squared sum of disparity differences (SSDD)) for the reconstruction of the 3-D channel geometry. The minimum of the energy function implicitly finds the epipolar lines by using the contributions along the feature curve, globally.

6.2 Sum of Squared Disparity Differences (SSDD)

We assume the images of left $(I_1(x,y))$ and right $(I_2(x,y))$ cameras are vertically translated v pixels and possibly rotated by angle ω around Y axis relative to each other. Vertical misalignment and rotation around Y axis are the crucial alignment in the case considered. The distance between cameras and discharges are higher that small measurement errors in Z, X directions will not cause difficulties in image matching. Also the cameras can be aligned correctly around X and Z axes using water levels.

An energy functional is defined by $E(v,\omega)$ and the solution for the correspondence problem by finding the v, ω, which minimizes the energy function.

$$\min_{v,\omega} E(v,\omega) = \min_{v,\omega} \sum_{i=1}^{n-1} \left(d_{v,\omega}^{i+1} - d_{v,\omega}^{i}\right)^2 \tag{6}$$

where $d_{v,\omega}^{i}$, $d_{v,\omega}^{i+1}$ are disparities at ith and $i+1$th features. It can be assumed that the slight vertical shift of the cameras gives a shift in y coordinates and the slight rotation ω around Y axis gives a shift in x coordinates in the images which is an error in the disparity measured.

To find the solution for vertical shift v, (6) can be written as

$$E(v) = \sum_{i=1}^{n-1} \left[\left(X_l^{v+i} - X_r^{i}\right) - \left(X_l^{v+i+1} - X_r^{i+1}\right) \right]^2 \tag{7}$$

where $X_l \in I_l$ and $X_r \in I_r$ are vectors of length n containing m feature points from the tortuous curves and $(n\text{-}m)$ feature points from the outside of the tortuous curves at the both ends of L and R images. The vectors X_r^i, X_r^{i+1}, X_l^{v+i} and X_l^{v+i+1} are the right feature vector, the shifted right feature vector, the left feature vector and the shifted left feature vector. The left feature vectors are shifted by v pixels respect to right feature vectors respectively. For discharge images, the feature contours are one pixel thickness curves, i.e., one sample per row of the image and can be expressed as vectors.

By expanding (7), if n>>1,

$$= \sum_{i=1}^{n-1} \left[\begin{array}{l} 2X_l^{v+i^2} + 2X_r^{i^2} - 4X_r^i X_l^{v+i} + 2X_r^i X_l^{v+i+1} \\ +2X_r^{i+1} X_l^{v+i} - 2X_l^{v+i} X_l^{v+1+i} - 2X_r^i X_r^{i+1} \end{array} \right] \tag{8}$$

Equation (8) shows that, when minimizing the expression, while it is maximizing the correlation of each image ($4X_r^i X_l^{v+i}$), it is simultaneously balanced by minimizing the correlation for a small shift in the images ($2X_r^i X_l^{v+i+1} + 2X_r^{i+1} X_l^{v+i}$), so that the energy function for the v yielding a global minimum. In the solution, the two covariance terms of neighboring pixels of the same image are balanced with two squares of image terms, ($2X_l^{v+i\,2} + 2X_r^{i\,2} - 2X_l^{v+i} X_l^{v+i+1} - 2X_r^i X_r^{i+1}$), essentially using the smoothness of the channel at the neighboring pixel.

In the case of sharp discontinuities in the depth, the disparity difference is higher. Here we propose that a penalty must be added at every discontinuity of the depth. The sign of the penalty and the amount of the penalty may be decided according to the direction and the length of the depth discontinuity. The penalty is η depending on the length of each discontinuity in the vector D_C. The vector D_C is containing depth discontinuity points along the channel.

$$E(v) = \sum_{i=1:N} \left[\left(X_l^{v+i} - X_r^i \right) - \left(X_l^{v+1+i} - X_r^{i+1} \right) \pm \eta(D_C) \right]^2 \tag{9}$$

In this approach, the discharge image feature contours are moved on each other and the energy function (4) is formed for each slide. The point at where the energy function obtain a minimum is selected as the matching points for the feature contours. The most likely disparity differences expected are (+1, 0, -1). However, at depth discontinuities and sharp curves the disparity difference tends to be large (>>1). In the discharge images the depth discontinuities are known by the light characteristics. Some peaks in the channel zone (excluding the channel ridge), indicate a depth discontinuity in the direction of the visual ray. This is important, almost *apriori* depth information, and can be incorporated in the stereo reconstruction. An additional penalty cost is proposed at the channel bright spots (Fig. 3(d)) to reduce the higher disparity difference, cf. (9). The amount of the penalty can be found by the light characteristics (3).

Fig. 9 shows the energy calculated using the equation (6) for the pair of images shown in Fig. 3. The energy is minimized at v = -10. The depth construction directly from the obtained minimizing point is shown in Fig. 14. *The minimized energy E is forced for the optimum continuation in the depth map.* A drawback of this method is that there are several local minima in the energy functional. The closest local minimum finds a nearby solution.

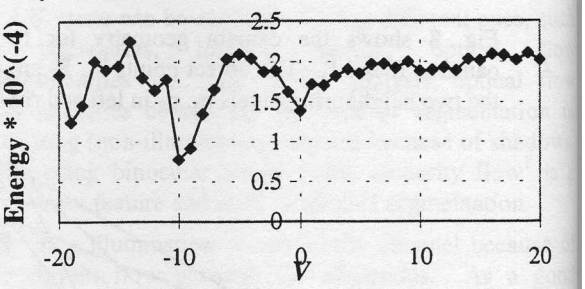

Fig. 9 The energy function versus v at each slide

7 Experimental Results

To demonstrate the ability of the algorithm to perceive the depth, the resulted depths using the binocular stereo images is compared with the depth using the orthogonal camera images (ground truth). Fig. 10 shows the set images from the experiment. Fig. 11 show the features extracted. The depth reconstructed using binocular stereo and orthogonal camera are shown in Fig. 12.

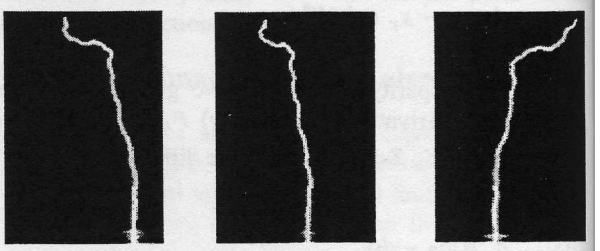

(a) Camera (b) Camera 2 (c) Camera 3

Fig. 10 The simultaneous images from experiment.

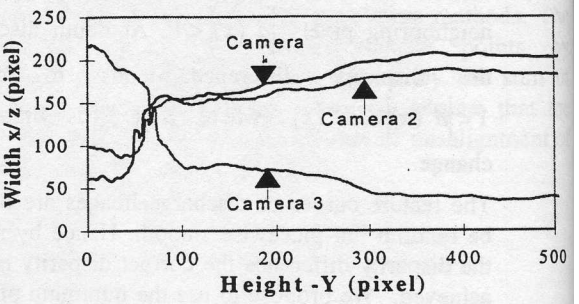

Fig. 11 The extracted features for the images in Fig. 10.

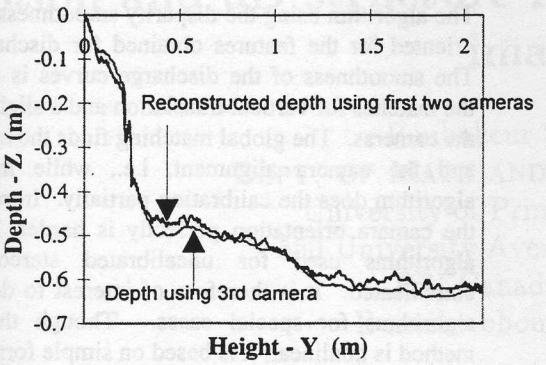

Fig. 12 The reconstructed depth for images in Fig. 10.

The set of images shown in Fig. 3 are taken for the example 2. The features extracted for the simultaneous images and the depth reconstructed are shown in Fig. 13 and Fig. 14 respectively.

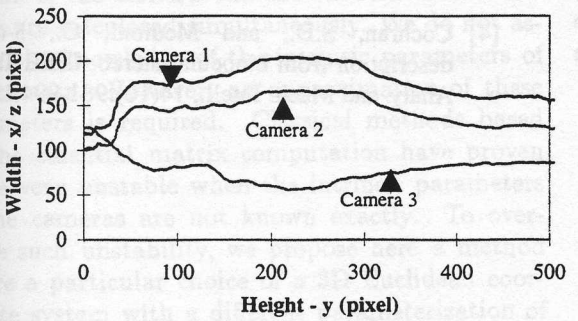

Fig. 13 The extracted features for images in Fig. 3

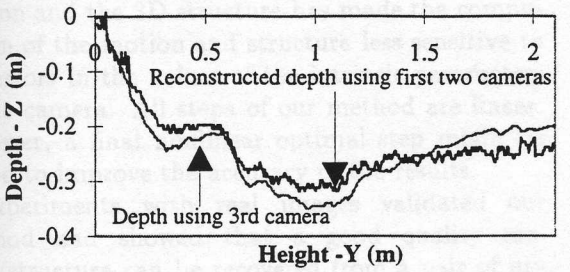

Fig. 14 The reconstructed depths for images in Fig. 3.

The constructed orthogonal view from the binocular camera images are shown with the 3rd camera images in Fig. 15. The 3-D shape of the discharges are reconstructed very well though the uncertainty in the feature points has given an error in the finer shape of the reconstructed depth.

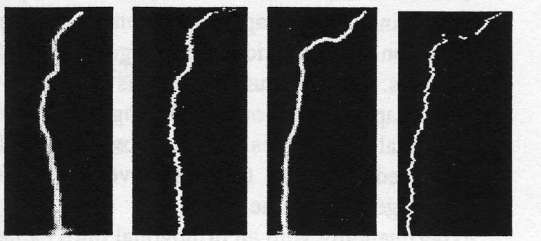

Fig. 15 Third camera images and reconstructed orthogonal views.

Experiment II: Lightning Flashes

Lightning imaging has been carried out over the Atlantic ocean from the west coast of the Denmark. Two electronic video cameras were focused over the sea from the sea-shore to record the lightning flashes. The base line of the cameras was 80 m. A corresponding pair of images and the computed relative depth are shown in Fig. 16, Fig. 17 respectively.

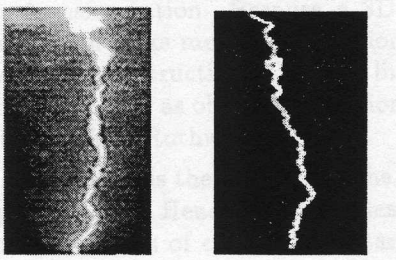

Fig. 16 Corresponding image pairs (Left and Right Images) of lightning images

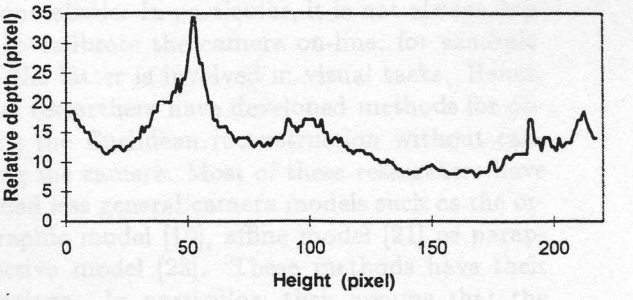

Fig. 17 The reconstructed depth map.

8 Conclusions

The work has addressed the problem of perceiving and measuring the shape orthogonal to the measuring direction of electrical discharges using two parallel cameras. The computation of this new view provides the 3-D shape(orientation), 3-D length and volume of the electrical discharges. It is shown that the algorithm presented recovers the shape very well for electrical discharges. The results have been verified experimentally with an orthogonal third camera view.

Stereo algorithms are sometimes non-trivial because of the correspondence problem. Reasons for this correspondence problem include the fact that the feature detection is not perfectly reliable, occluded features appear in one image in wide angle stereo and light differences exist at conjugate pixels because of source directions. For discharge images, it is shown that the establishment of matches is clear along the highly illuminated current path. Also, it is shown that at depth discontinuities, unlike reflecting objects, the light is additive, giving a priori knowledge to add a penalty at the discontinuity points in disparity difference terms in the image matching algorithms.

The algorithm using the disparity smoothness is problem-oriented for the features obtained for discharge images. The smoothness of the discharge curves is used to find the matches for vertical translation and a slight rotation of the cameras. The global matching finds the epipolar lines and the camera alignment, i.e., while matching the algorithm does the calibration partially. In reality, fixing the camera orientation perfectly is harder. Most of the algorithms used for uncalibrated stereo are very complicated. It is therefore of interest to derive simple algorithms for special cases. Though the presented method is nonlinear, it is based on simple formulas.

9 References

[1] Faugeras, O., Three Dimensional Computer Vision, Cambridge, MIT, 1993.

[2] Horn, B. K. P., Robot Vision, MIT Press, 1986.

[3] Uman, M. A., The Lightning Discharge, International Geo. Phy., pp. 99-107, 192, 193, Vol. 39, 1987.

[4] Cochran, S.D., and Medioni, G., 3-d surface description from binocular stereo. IEEE Trans. Patt. Analy. and Mach. Intell., 14(10):981-994,1992.